International Journal of Nanomedicine

Dovepress
Taylor & Francis Group

Open Access Full Text Article

ORIGINAL RESEARCH

Carbonic Anhydrase IX Targeted Polyaspartamide fluorescent Probes for Tumor imaging

Yu Zhang[1,2,*], Fan Liu[2,3,*], Chuntao Shao[2,*], Jun Huang[3], Guoping Yan[1]

[1]College of Chemical and Material Engineering, Quzhou University, Quzhou, Zhejiang Province, 324000, People's Republic of China; [2]School of Materials Science and Engineering, Wuhan Institute of Technology, Wuhan, 430205, People's Republic of China; [3]School of Chemical and Biomolecular Engineering, University of Sydney, NSW, 2006, Australia

*These authors contributed equally to this work

Correspondence: Guoping Yan, Tel +86 570 8028560, Email guopingyan@qzc.edu.cn

Background: Precise intraoperative tumor delineation is essential for successful surgical outcomes. However, conventional methods are often incompetent to provide intraoperative guidance due to lack specificity and sensitivity. Recently fluorescence-guided surgery for tumors to delineate between cancerous and healthy tissues has attracted widespread attention. The contrast-enhanced fluorescent imaging has been applied for non-invasive diagnosis of cancers using tumor-targeting fluorescent probes.

Methods: The carbonic anhydrase IX targeted polyaspartamide fluorescent compounds (SD-PHEA-NI) were synthesized by incorporating a tumor-targeting group of sulfadiazine (SD) and N-butyl-4-ethyldiamino-1,8-naphthalimide (NI) into water-soluble carriersof poly-α,β-[N-(2-hydroxyethyl)-L-aspartamide] (PHEA). These derivatives were also characterized by Fourier transform infrared spectroscopy, gel permeation chromatography, ultraviolet-visible spectroscopy, nuclear magnetic resonance spectroscopy and fluorescence assays. The cellular uptake, cytotoxicity, and fluorescence imaging ability were evaluated.

Results: Experiment results indicated that SD-PHEA-NI has low cytotoxic to Henrietta Lacks (HeLa) cells. Moreover, B16F10 melanoma cells can take up SD-PHEA-NI and show good green fluorescent images. However, SD-PHEA-NI displayed a low-intensity green fluorescence signal in healthy human embryonic kidney (293T) cells.

Conclusion: SD-PHEA-NI can be considered a potential fluorescent probe for the detection of tumors. This study has the potential to enhance tumor diagnosis and image-guided surgical interventions by providing real-time information and robust decision support, thereby reducing recurrence and complication rates and ultimately improving patient outcomes.

Keywords: fluorescent imaging, polyaspartamide, sulfadiazine, naphthalimide, fluorescent probes

Introduction

Renal cell carcinoma (RCC) originates from renal tubular epithelial cells and is responsible for approximately 90% of all renal malignancies.[1–3] Due to the deep location of the kidney, the early clinical manifestations of RCC are insidious, and the patients exhibit no obvious symptoms. More than 16% of patients develop distant metastasis at the time of the initial diagnosis.[4,5] Surgical resection is currently the main treatment method, but the surgeon mainly relies on visual inspection, palpation and subjective experience to distinguish between malignant lesions and adjacent (healthy) tissues. The unclear boundary of the lesion leads to incomplete tumor resection, increases the risk of recurrence, and ultimately affects the patient's postoperative prognosis and survival rate.[6,7] Therefore, accurate assessment of the resection margin during surgery is crucial for diagnosis, staging and ultimate patient prognosis.

Fluorescence imaging (FI) has emerged as a promising technique for intraoperative management of tumor margins owing to its advantages, including real-time feedback, high specificity, high sensitivity, and ionizing radiation-free, as well as low cost.[8–10] Currently, fluorescent probes have been used for in vivo imaging and differentiation of normal tissue and tumor tissue, including small-molecule probes, nanoparticle-based probes, and quantum dots.[11–13] Small-molecule probes, such as indocyanine green (ICG) and 1.8-naphthalimide, are widely applied in FI to improve

Received: 25 October 2024
Accepted: 3 January 2025
Published: 15 January 2025

contrast and sensitivity.[11,14] In particular, polymeric nanoparticles (PNs) have demonstrated significant potential in drug delivery, improved biocompatibility and the ability to be easily functionalized. At present, some polymeric nanoparticles labeled with tumor-targeting molecules have been reported to effectively deliver fluorescent probes to the tumor regions. These systems can increase the imaging efficacy for tumors and improve the half-life, solubility, and stability, which dramatically reduces potential side effects in the body.[15,16] In general, a fluorescent probe is chemically attached to polymer biomaterials,[17] such as polylysine and poly(acrylic acid). The encapsulating materials including liposomes, polymersomes, polymeric nanoparticles, and micelles.[18,19] Glycol chitosan-based polymeric nanoparticles have been investigated to develop therapeutic drugs and fluorescent agents for tumor accumulation and treatment.[20]

As a water-soluble synthetic protein-like polymer, polyaspartamide possesses nontoxic, nonantigenic, good biocompatibility and degradability, and then can be easily modified through side chain groups. The degradation products of poly(amino acid)-based biomaterials are nontoxic small-molecule nutrients, which can be used or excreted by physiological processes in the body. So it is widely applied as a plasma extender and drug delivery carrier.[21,22] Some polymer pro-drugs were produced by a covalent link of anti-inflammatory agents and antiviral drugs with poly-α,β-[N-(2-hy droxyethyl)-D,L-aspartamide] (PHEA). They indicated increased drug stability, solubility, and bioavailability. Tumor-targeting polymer MRI contrast agents were made by incorporating gadolinium diethylenetriamine-pentaacetic acid (Gd-DTPA) into PHEA. Therefore, PHEA can be used as an ideal polymer carrier for fluorescent probes.[23,24]

Currently, contrast-enhanced FI has attracted wide interest in non-invasive detection of cancers. However, some probes are restricted to tumor imaging due to no tumor-targeting biodistribution. Moreover, tumor-targeting fluorescent probes can be used to effectively monitor targeted molecular imaging by the conjugation of fluorescent probes with tumor-targeting molecules, such as peptides,[15,25] folate,[26,27] antigens,[28] and cell surface receptors.[29]

Carbonic anhydrase (CA IX) is notably over-expressed in clear cell RCC and is often used as a biomarker for this type of cancer due to its high specificity and correlation with tumor aggressiveness.[30,31] Therefore, the design and construction of ultrasonic molecular probes targeting CA IX can realize targeted molecular imaging of RCC. Sulfadiazine (SD) derivatives are known for their high specificity for transmembrane carbonic anhydrase (CA) isoforms, cost-effectiveness, and broad availability, and then are developed as tumor-targeting moieties in anticancer drug formulations. Some SD derivatives can accumulate into Walker carcinoma or Yoshida sarcoma to treat cancers and suppress metastasis.[32,33] SD-conjugated Gd-DTPA derivatives demonstrated high uptake by Hepatoma and Ehrlich ascites carcinoma cells in mice. SD-containing PHEA gadolinium complexes showed high uptake and enhanced MRI in hepatomas.[24,34]

Naphthalimide derivatives are usually applied as organic dyes, luminophores, and anticancer agents due to their good photophysical and chemical property.[35,36] To enhance the accuracy of intraoperative fluorescent probes using water-soluble carriers, this study introduces a carbonic anhydrase IX targeted polyaspartamide fluorescent probes (NI-PHEA-SD). This probe incorporates a carbonic anhydrase IX-targeting group of sulfadiazine (SD) and N-butyl-4-ethyldiamino-1,8-naphthalimide (NI) into water-soluble carriers of poly-α,β-[N-(2-hydroxyethyl)-L-aspartamide] (PHEA). The probe responds specifically to over-expressed carbonic anhydrase IX, enabling precise localization of renal cell carcinoma during surgery. Tumor lesions smaller than 1 mm in diameter can be accurately identified using PHEA-NI-SD and completely excised under fluorescence imaging guidance.

Materials and Methods

Materials

Polysuccinimide (PSI),[24,34] sodium sulfadiazine (SDNa),[24] NI,[35,36] and PHEA[24,34] were synthesized using previously reported methods cited in the literatures. Human embryonic kidney (293T) cells, B16F10 mouse melanoma cells, and Henrietta Lacks (HeLa) cells were provided by the China Center for Type Culture Collection of Wuhan University, China, and cultured according to a previously described method.[37]

Synthesis of Polyaspartamide Containing SD and NI Groups (SD-PHEA-NI)

Polysuccinimide (PSI, 0.97g, 10 mmol) was dissolved in N,N-dimethylformamide (DMF, 10mL) and N-butyl-4-ethyl-diamino-1,8-naphthalene imide (NI,1.24g, 0.2mmol, 0.4 equiv. to the repeat structure units of PSI) was added to the solution with rapid stirring at room temperature. The reaction solution was continued with stirring for 48h at 80°C and further cooled to room temperature. Subsequently, the solution of ethanolamine (1 mL, 18 mmol, 1.8 equiv. to the repeating structural units of PSI) in DMF (3mL) was added to the reaction solution with rapid stirring at 0°C. The reaction mixture was stirred continuously for 4h at 0°C and more for 12h at room temperature. The resulting mixture was filtered and precipitated using a solution of dichloromethane and n-hexane (V/V, 2/1). The precipitate was collected from filtration and dried under vacuum. The residual solid was dissolved with distilled water in a dialysis bag and dialyzed against distilled water for 48 h. After filtration, the dialyzed solution was evaporated, and the solid residue was dried under vacuum to producepolyaspartamide containing naphthalene imide groups (PHEA-NI) (1.59g, 71%).

PHEA-NI (0.97g, 10 mmol) and triethylamine (200 μL) were dissolved in DMF (10 mL) and bromoacetyl bromide (130.5μL, 0.87 mmol, 0.51 equiv. for the repeat structural units of PSI or 76.8 μL, 0.51 mmol, 0.3 equiv. to the repeat structure units of PSI) was added, respectively, to the solution with rapid stirring at 0°C. The reaction was continued with stirring for 3 h at 0°C and more for 1 h at room temperature. Most of the solvent was removed under vacuum, and the resultant mixture was precipitated with a solution of dichloromethane and n-hexane (V/V, 2/1). The solid residue was reprecipitated from DMF against dichloromethane and n-hexane, filtered and dried under vacuum to obtain a solid (Br-PHEA-NI (I): 0.72 g, 73%, or Br-PHEA-NI (II): 0.8 g, 83%).

Br-PHEA-NI (0.66g, 2 mmol) was dissolved in N,N-dimethylformamide (DMF, 10 mL). SDNa (I:, 0.56 g, 2mmol, or II: 0.41 g, 1.5 mmol) and tetrabutyl ammonium hydroxide (1 mL) were added, respectively, to the solution with rapid stirring at room temperature. The reaction was continued with stirring for 48h.The resulting mixture was filtered and precipitated using a solution of dichloromethane and n-hexane (V/V, 2/1). After filtration, the precipitate was collected and dried under vacuum to produce a solid. The solid was dissolved with distilled water in a dialysis bag and dialyzed against distilled water for 48 h. After filtration, the dialyzed solution was evaporated and the solid residue was dried under vacuum to give polyaspartamide containing sulfadiazine and naphthalene imide groups (SD-PHEA-NI) (L_1:0.79g, 84% or L_2:0.65 g, 83%). The average molecular weight (Mn) was measured using Gel Permeation Chromatography (GPC). SD-PHEA-NI (L_1): ^{1}H NMR (DMSO-d_6, δ ppm): 8.25, 6.55 (CH, sulfadiazine), 7.47 (CH, naphthalene ring), 4.63 ($OCCH_2N$), 3.89, 3.36, 3.15, 2.68, 2.51 (CH_2, CH), 1.55, 1.29, 0.89 (CH_3); Mn: 1.59×10^4, Polydispersity: 1.15; FT-IR (KBr, ν_{max}, cm^{-1}): 3419 (-OH), 2930 (C-H), 1669, 1510 (CO-NH), 1385 (C-N), 1120 (SO_3), 910, 770, 669 (C_6H_4); UV (H_2O,λ_{max}, nm): 266, 286, 439.

SD-PHEA-NI (L_2): ^{1}H NMR (DMSO-d_6, δ ppm): 8.25, 6.57 (CH, sulfadiazine), 7.47 (CH, naphthalene ring), 4.61 ($OCCH_2N$), 3.89, 3.42, 3.14, 2.66, 2.51 (CH_2, CH), 1.53, 1.29, 0.89 (CH_3); Mn: 1.82×10^4, Polydispersity: 1.19; FT-IR (KBr, ν_{max}, cm^{-1}): 3448 (-OH), 2928 (C-H), 1664, 1507 (CO-NH), 1385 (C-N), 1121 (SO_3), 910, 771, 668 (C_6H_4); UV (H_2O, λ_{max}, nm): 266, 286, 439.

Vitro Cytotoxicity Assay

HeLa cells (2×10^5/mL) were plated in 96 wells plates in the RPMI-1640 medium supplemented with 10% fetal bovine serum (Gibco). Co., USA, 100 μg/mL streptomycin and 100 units/mL penicillin) and the number of cells in each well was 2×10^4. The cells were incubated for 24 h in an incubator (37°C, 5% CO_2), and residual liquid was then removed and the solution of polyaspartamide containing sulfadiazine and naphthalene imide groups (SD-PHEA-NI: L_1, L_2, 100 μL)in growth medium was added. After a 48h incubation, thiazolyl blue (3-[4,5-dimethylthiazol-2-yl]-2,5-diphenyltetrazolium bromide (MTT, 20μL, 5.0 mg/mL) solution in phosphate-buffered saline (PBS) was added to each well. The cells were incubated again for 4h. After removal of growth medium, dimethyl sulfoxide (DMSO, 100μL) was added and the solution shaken for 30 min. The absorbance (optical density: OD_{492}) was measured at 492 nm using a DG-3022A ELISA-Reader (Hercules, CA, United States) and expressed as a percentage relative to control cells (no SD-PHEA-NI).

Fluorescent Imaging Assay in Healthy Cells

Human embryonic kidney cells (293T; 2×10^5/mL) were implanted in 6-well plates (1×10^5/mL) in DMEM (10% fetal bovine serum, 100 units/mL penicillin and 100 μg/mL streptomycin). The cells were incubated for 24 h in an incubator (37°C, 5% CO_2). After separation of growth medium, pure growth medium or the solution of SD-PHEA-NI (L_1, L_2 or PHEA-NI, 1 mL, 100 μg/mL) in growth medium was added, respectively. After 2h of incubation, the residual liquid was moved again, and the cells were rinsed with PBS three times. Subsequently, the cells were fixed with paraformaldehyde (0.5 mL, 4%) for 10 min and stained with benzophenone imine (Hoechst, 5 μg/mL) for more 10 min. The cell morphology and density were observed using a confocal laser scanning microscope (CLSM) (TCS SP8, Leica, Germany).

Fluorescent Imaging in Tumor Cells

B16F10 cells (1×10^5/mL) were implanted in 6 wells plates in DMEM (100 units/mL penicillin,10% fetal bovine serum and 100 μg/mL streptomycin). The cells were incubated for 48 h in an incubator (37°C, 5% CO_2). After separation of growth medium, pure growth medium or the solution of SD-PHEA-NI (L_1 or L_2, 1 mL, 100 μg/mL) in the growth medium was added, respectively. After 2h of incubation, residual liquid was moved again and the cells were rinsed with PBS three times. Subsequently, the cells were fixed with paraformaldehyde (0.5 mL, 4%) for 10 min and stained with 4',6-diamidino-2-phenylindole (DAPI, 5 μg/mL) for more 10 min. The cell morphology and density were observed using a confocal laser scanning microscope (CLSM) (TCS SP8, Leica, Germany).

Cellular Uptake Test

B16F10 melanoma cells (1×10^5/mL) were implanted in 24 wells plates in RPMI-1640 media (100 units/mL penicillin, 100 μg/mL streptomycin and 10% fetal bovine serum (Gibco). Co., USA)). The cells were incubated for 24 h in an incubator (37°C, 5% CO_2). After removal of growth medium, 200 μL of pure growth medium or growth

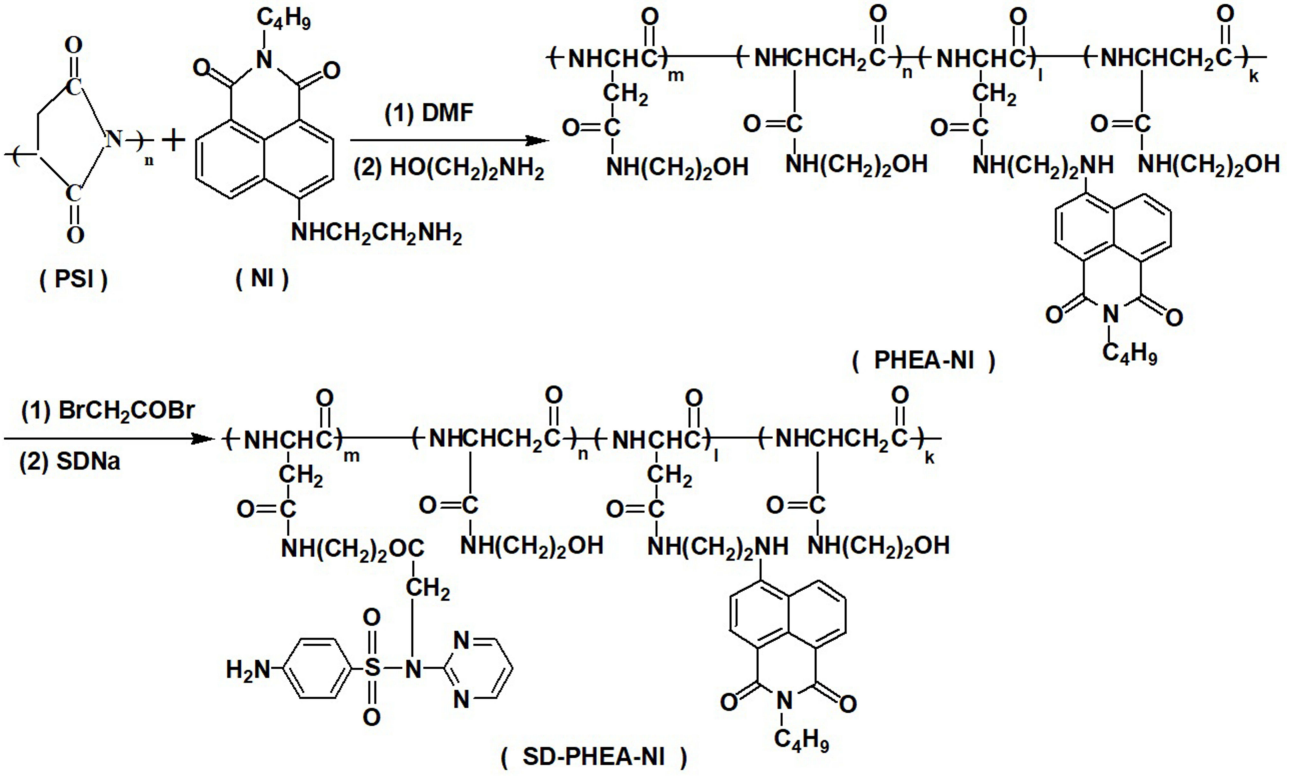

Scheme 1 Synthetic route to polyaspartamide fluorescent probes containing naphthalimide and sulfadiazine groups (SD-PHEA-NI).

medium containing SD-PHEA-NI (0.25 μmol/L) was added, respectively. After a 2-h incubation, the growth medium was removed again, and the cells were washed three times with PBS and subsequently fixed with paraformaldehyde (0.5mL, 4%) for 10 min. The cell morphology and density were observed using an IX-70 inverted fluorescence microscope (Olympus Co., Ltd., Japan).

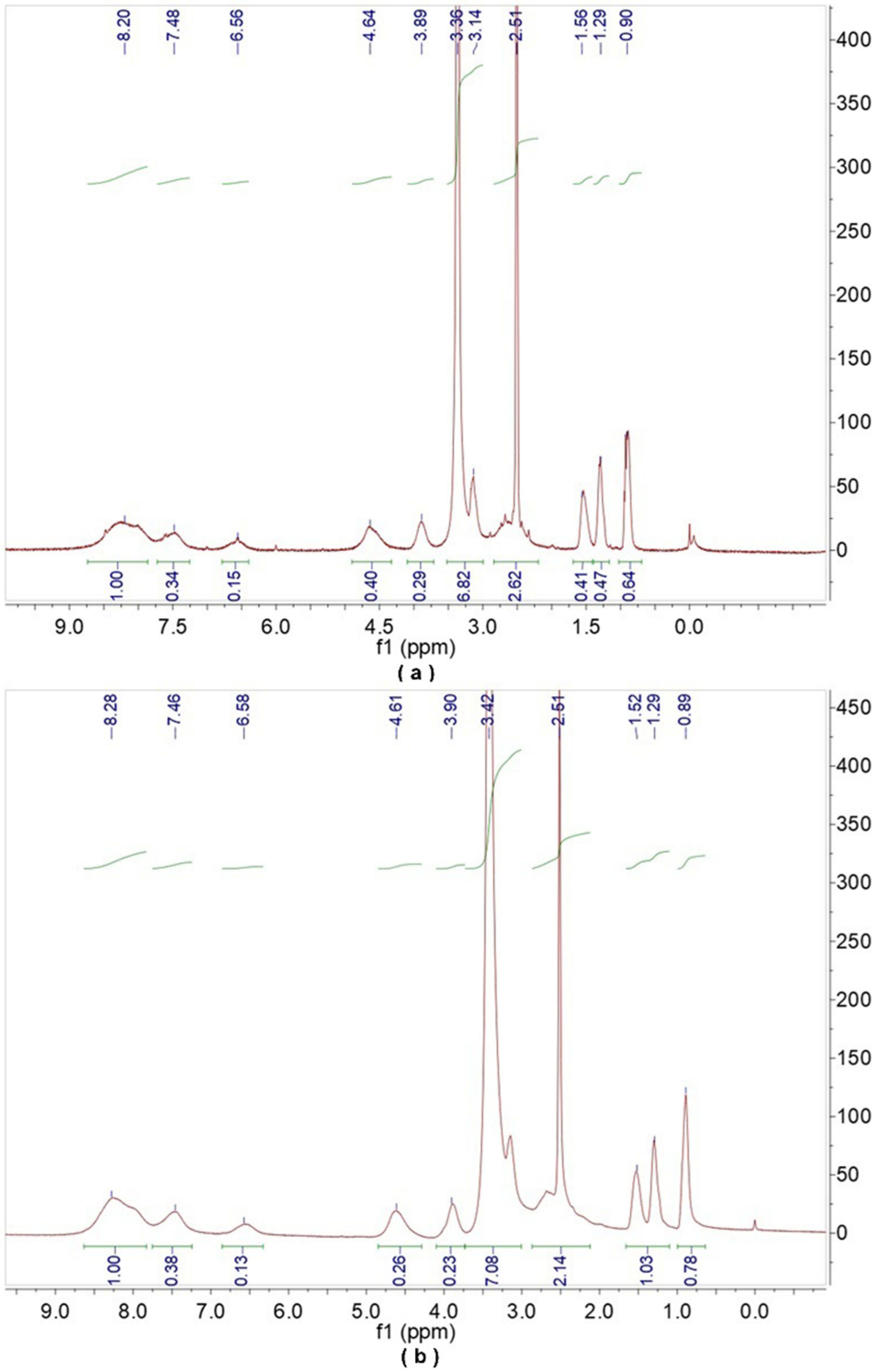

Figure 1 ^{1}H NMR spectra of SD-PHEA-NI (L_1: a and L_2: b).

https://doi.org/10.2147/IJN.S500614

An inhibited cell uptake assay was performed according to the method described above. B16F10 melanoma cells (1×10^5/mL) were implanted in 24 wells plates in RPMI-1640 media. The cells were incubated for 24 h in an incubator (37°C, 5% CO_2). After removal of growth medium, growth medium containing SD (25 μmol/L, 200 μL) was added and then incubated for 1 h in an incubator (37°C, 5% CO_2). After removal of growth medium, a solution of SD-PHEA-NI (0.25 μmol/L, 200 μL) in growth medium was added and incubated for 2 h. The growth medium was removed again, and then the cells were washed three times with PBS and subsequently fixed with paraformaldehyde (0.5mL, 4%) for 10 min. The cell morphology and density were observed using an IX-70 inverted fluorescence microscope.

Results and Discussion

Synthesis and Characterization

Two polyaspartamides containing sulfadiazine and naphthalimide groups (SD-PHEA-NI: L_1, L_2) were synthesized by the incorporation of fluorescence molecule NI and tumor-targeting group sulfadiazine into a polyaspartamide carrier (Scheme 1). The experimental data from UV, FT-IR,^{1}H NMR, GPC and fluorescenctspectra provided evidence for the formation of SD-PHEA-NI (Figures 1–5).

^{1}H NMR spectra of SD-PHEA-NI (L_1, L_2) displayed typical peaks of sulfadiazine and naphthalimide groups, which appeared at 8.25, 6.55, 1.55–0.89 ppm, and 7.47 ppm, respectively (Figure 1a and b), which indicated that SD and NI were covalently bound to polyaspartamide, respectively. The average grafted mole ratios of SD and NI groups

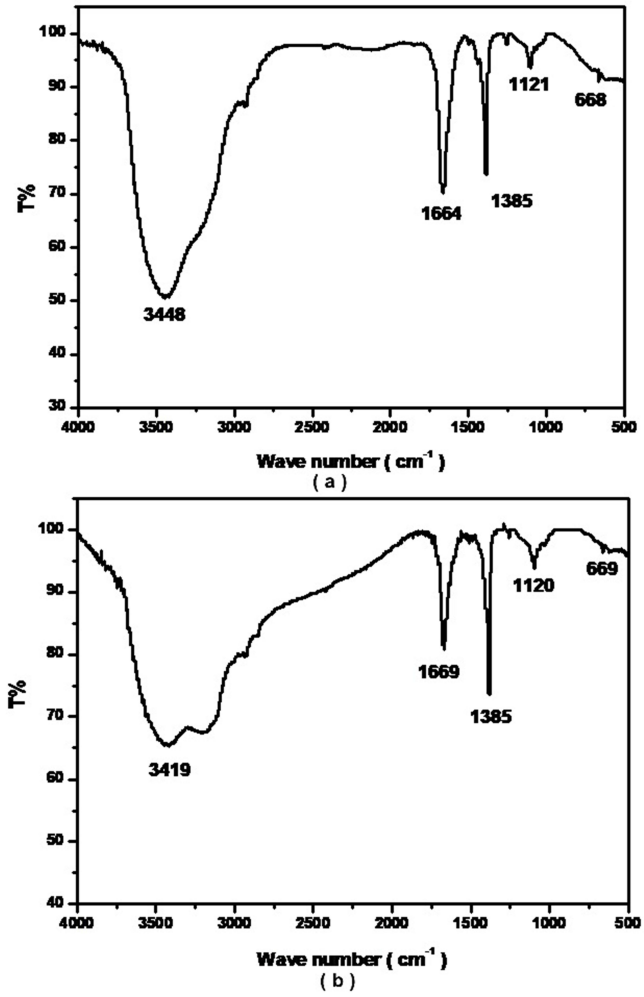

Figure 2 IR spectra of SD-PHEA-NI (L_1: a and L_2: b).

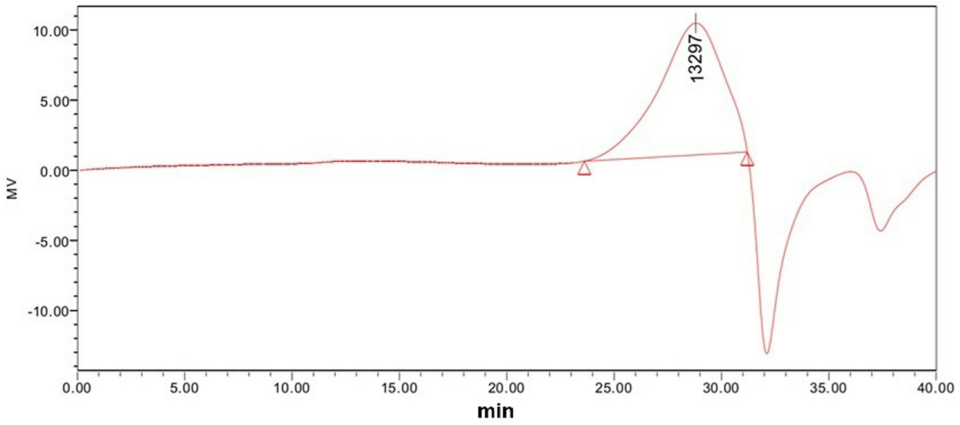

Mn (Da)	Mw (Da)	MP (Da)	Mz	Mz+1 (Da)	PDI
15963	18447	13297	21861	21861	1.16

(a)

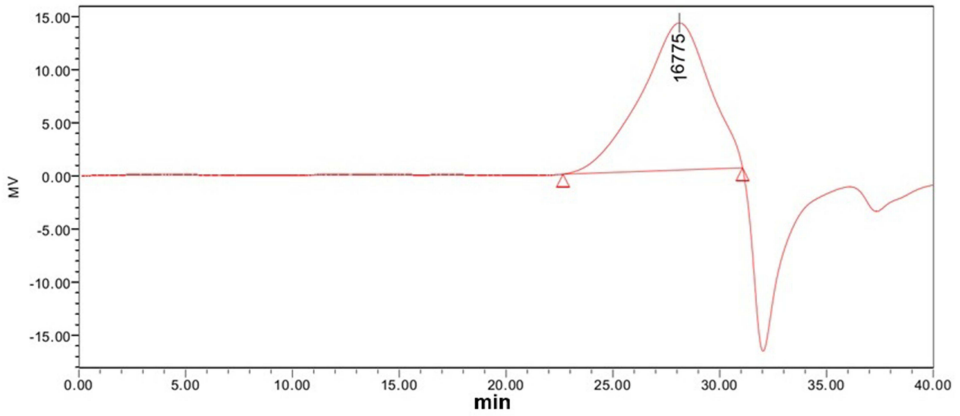

Mn (Da)	Mw (Da)	MP (Da)	Mz	Mz+1 (Da)	PDI
18240	21722	16775	26425	32106	1.19

(b)

Figure 3 GPC spectra of SD-PHEA-NI (L_1: a and L_2: b).

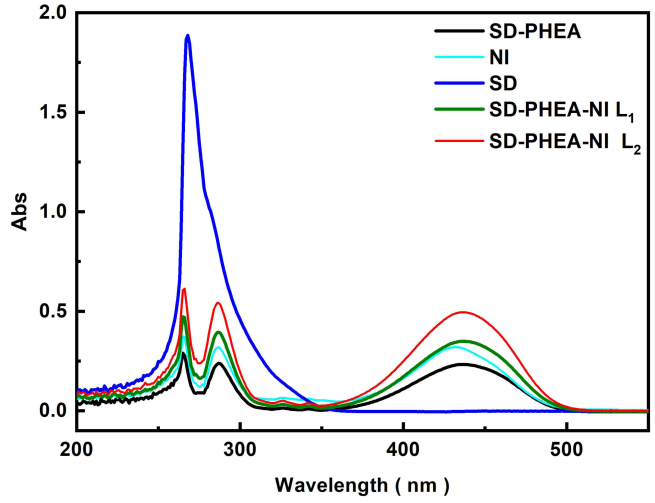

Figure 4 UV of polyaspartamide fluorescent probes (SD-PHEA-NI).

https://doi.org/10.2147/IJN.S500614

topolyaspartamide (mol%) in SD-PHEA-NI (L_1, L_2) molecules were: L_1,7.6% and 16%, and L_2,5.4% and 18.2%, respectively.

IR spectra of SD-PHEA-NI (L_1, L_2) showed characteristic absorption peaks of amide bonds (CONH) at 1669–1507 cm^{-1}, amino groups (NH) at 3448–3419 cm^{-1}, and benzyl groups varying from 910 to 668 cm^{-1}, respectively (Figure 2a and b), which demonstrated that both SD and NI were covalently bound to PHEA. SD-PHEA-NI (L_1, L_2) had number-average molecular weights (Mn) of $1.59\times10^4$and 1.82×10^4, respectively (Figure 3a and b).

UV spectra indicated that SD-PHEA-NI had the same characteristic absorption peaks (266, 286 nm: SD, and 439 nm: NI) as those of SD and NI (Figure 4). The fluorescent spectra showed that SD-PHEA-NI (L_1, L_2) had a maximum excitation wavelength of 437 nm and maximum emission wavelength of 525 nm (Figure 5). It appears that SD-PHEA-NI possesses the similar typical fluorescence emission wavelength to NI. Therefore, SD-PHEA-NI (L_1, L_2) retains the same photophysical property as NI for fluorescent imaging. Moreover, they should possess good tumor-targeting property to achieve highly sensitive enhanced imaging of tumor cells.

Vitro Cytotoxicity

The growth and metabolism of HeLa cells incubated with SD-PHEA-NI (L_1, L_2) are shown in Figure 6. At a concentration (1 μg/mL) of the solution of SD-PHEA-NI (L_1, L_2), the viability of HeLa cells incubated with SD-

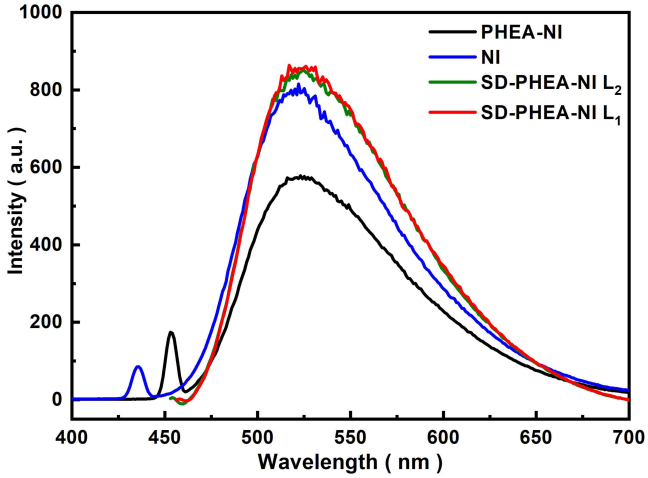

Figure 5 Fluorescent spectra of polyaspartamide fluorescent probes (SD-PHEA-NI).

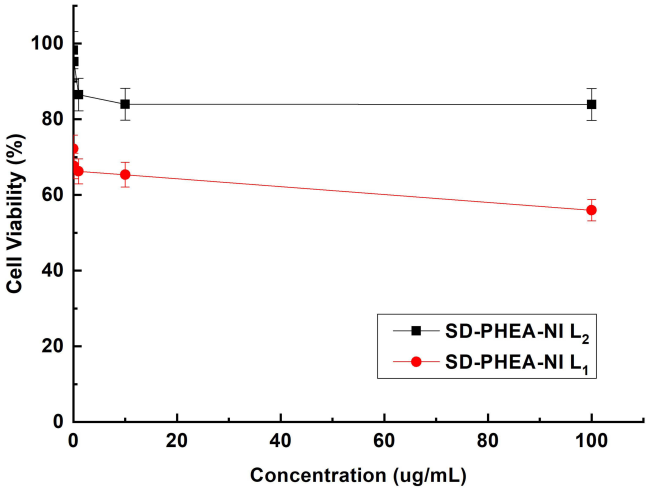

Figure 6 In vitro cytotoxicity of SD-PHEA-NI (L_1, L_2) to HeLa cells.

 https://doi.org/10.2147/IJN.S500614

PHEA-NI (L_1, L_2) was 66.3% and 86.5%, respectively. At a concentration (100 μg/mL) of the solution of SD-PHEA-NI, the viability of HeLa cells incubated with SD-PHEA-NI (L_1, L_2) was 56% and 83.9%, respectively. This illustrates that SD-PHEA-NI (L_1, L_2) exhibited low cytotoxicity in HeLa cells.

Sulfadiazine (SD) is an antibacterial and anti-inflammatory drug used clinically. SD-PHEA-NI (L_1, L_2) possessed high uptake and good tumor-targeting properties for tumor cells. SD-PHEA-NI (L_1, L_2) may selectively accumulate in HeLa cells and exhibit high anticancer efficiency to HeLa cells during increasing of incubation concentration. Moreover, SD-PHEA-NI (L_1) had slightly higher cytotoxicity to HeLa cells than that of SD-PHEA-NI (L_2) because the content of the SD groups attached to SD-PHEA-NI (L_1) was larger than that of SD-PHEA-NI (L_2).

Fluorescent Imaging

Fluorescent imaging of healthy 293T cells and B16F10 melanoma cells cultured with SD-PHEA-NI (L_1, L_2) is shown in Figures 7 and 8, respectively, when excited by white and blue light (excitation wavelength: 450 nm). Healthy 293T cells cultured with SD-PHEA-NI (L_1, L_2) and PHEA-NI displayed a low-intensity green fluorescent image when excited by blue light (Figure 7) because 293T cells present a rather low expression of transmembrane CA isoforms and cannot show high uptake of SD-PHEA-NI (L_1, L_2). Meanwhile, the cells cultured in growth medium did not show fluorescence when excited by blue light.

B16F10 cells cultured with SD-PHEA-NI (L_1, L_2) exhibited good green fluorescence images when excited with blue light (Figure 8). However, the cells cultured with pure growth medium showed good growth conditions when excited by white light, but no fluorescent images when excited by blue light. Moreover, SD-PHEA-NI (L_1, L_2) exhibited better fluorescence properties than PHEA-NI without a tumor-targeting group in B16F10 cell imaging. It is likely that these cells express high levels of transmembrane CA isoforms, which induce SD-PHEA-NI (L_1, L_2) to proactively accumulate

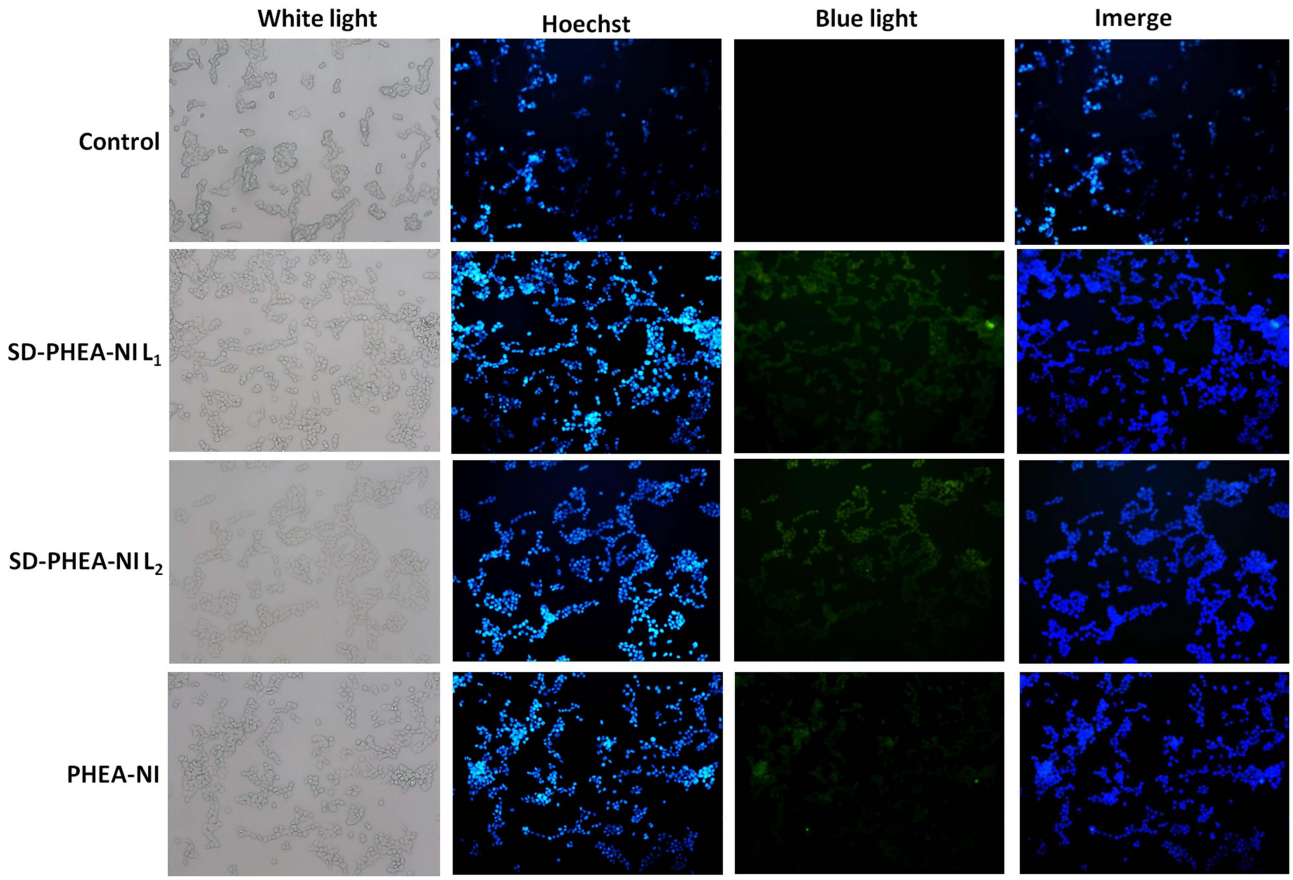

Figure 7 Fluorescent imaging of SD-PHEA-NI (L_1, L_2) to healthy 293T cells.

https://doi.org/10.2147/IJN.S500614

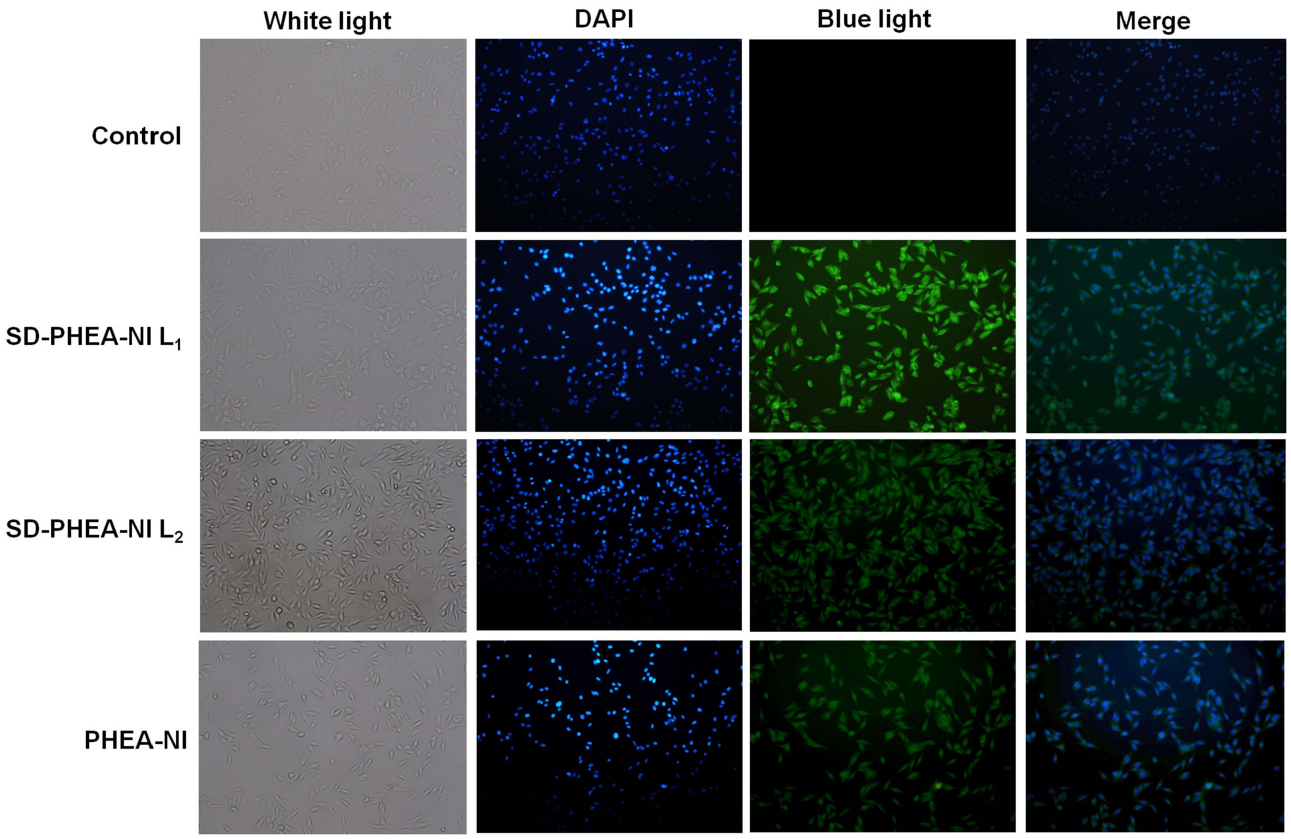

Figure 8 Fluorescent imaging of SD-PHEA-NI (L_1, L_2) to B16F10 cells.

in B16F10 cells mediated by the receptors. Therefore, SD-PHEA-NI (L_1, L_2) displayed high uptake by B16F10 cells due to SD groups of tumor-targeting property.

Cellular Uptake

Cell uptake assays of SD-PHEA-NI (L_2) were evaluated in B16F10 melanoma cells because SD-PHEA-NI (L_2) was less cytotoxic than SD-PHEA-NI (L_1). Fluorescence imaging of B16F10 cells incubated with SD-PHEA-NI (L_2) is shown in Figure 9 when excited by white and blue light (excitation wavelength: 450 nm). B16F10 cells incubated with SD-PHEA-NI (L_2) displayed good green fluorescence images when excited with blue light (Figure 9: B2). However, B16F10 cells incubated with pure growth medium indicated no fluorescence imaging when excited by blue light (Figure 9: B1).

In the inhibited cell uptake assay, B16F10 cells were incubated with SD solution for 1 h and subsequently SD-PHEA-NI (L_2, 0.25 μmol/L) solution later. B16F10 cells indicated the decreased intensity of green fluorescence imaging when excited by blue light (Figure 9: B3). The probable reason is that the transmembrane CA isoforms in tumor cells was covered up early by SD. So the tumor cells cannot take up SD-PHEA-NI (L_2)again and show an obvious decrease in fluorescence intensity after earlier inhibition of SD.

The comparable experimental values demonstrated that SD-PHEA-NI displayed good tumor-targeting property and characteristic green fluorescence imaging in B16F10 cells, whereas SD-PHEA-NI possessed a high specific selective behavior to B16F10 cells. Moreover, SD-PHEA-NI was selectively taken up by receptor-binding affinity between SD groups and the transmembrane CA isoforms.

Conclusions

Polyaspartamides containing sulfadiazine and naphthalene imide groups (SD-PHEA-NI) displayed similar UV and fluorescence property to NI. Moreover, SD-PHEA-NI exhibited low cytotoxicity to HeLa cells, high uptake and good

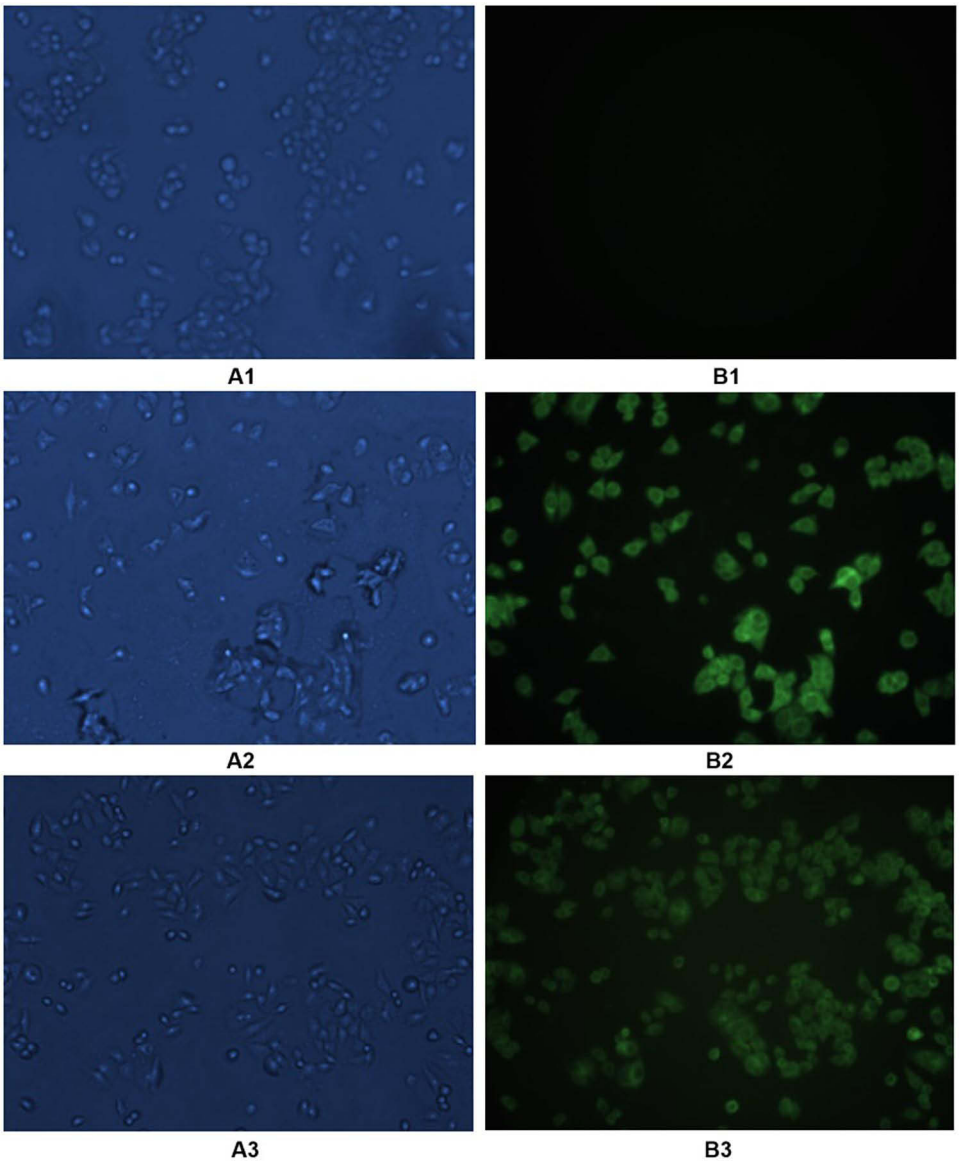

Figure 9 Inhibited fluorescence imaging of SD-PHEA-NI (L_2) to B16F10 cells. (A1 and B1: Control B16F10 cells excited by white light and blue light, respectively; A2 and B2: B16F10 cells incubated with SD-PHEA-NI (L_2) excited by white light and blue light, respectively; A3 and B3: B16F10 cells that were previously incubated by SD (25μmol/L) for 1h and subsequently incubated with SD-PHEA-NI (L2) (0.25μmol/L) later excited by white light and blue light, respectively.).

green fluorescence imaging in B16F10 cells. Therefore, SD-PHEA-NI can be considered a potential probe for targeted fluorescent imaging in tumors.

Data Sharing Statement

Data will be made available on request.

Acknowledgments

The authors are grateful to the National Natural Science Foundation of China (Grant No.52303132), Key Project of Zhejiang Province Natural Science Foundation (Grant No. LQZSZ25E030004), Key Science and Technology Projects of Quzhou City (Grant No. 2024K132), Hubei Province Natural Science Foundation for Youths (Grant No.2022CFB710), and Frontier Project of the Application Foundation of Wuhan Former Funded Science and Technology Program (Grant No. 2020020601012252), Hubei Province, China.

Disclosure

The authors report no conflicts of interest in this work.

References

1. Siddiqi A, Rani M, Bansal P, Rizvi MMA. Renal cell carcinoma management: a step to nano-chemoprevention. *Life Sci*. 2022;308:120922. doi:10.1016/j.lfs.2022.120922
2. Matthew Y, Francesca JS, Luis B, et al. Renal cell carcinoma. *Lanet*. 2024;404(10451):476–491.
3. Gray RE, Harris GT. Renal cell carcinoma: diagnosis and management. *Am Fam Physician*. 2019;99(3):179–184.
4. Bahadoram S, Davoodi M, Hassanzadeh S, Bahadoram M, Barahman M, Mafakher L. Renal cell carcinoma: an overview of the epidemiology, diagnosis, and treatment. *G Ital Nefrol*. 2022;39(3)::2022–vol3.
5. Zhong C, Chen J, Ling Y, et al. Indocyanine green-loaded nanobubbles targeting carbonic anhydrase IX for multimodal imaging of renal cell carcinoma. *Int J Nanomed*. 2023;18:2757–2776. doi:10.2147/IJN.S408977
6. Feng Y, Yan H, Mou X, et al. A dual-cascade activatable near-infrared fluorescent probe for precise intraoperative imaging of tumor. *Nano Lett*. 2024;24(20):6131–6138. doi:10.1021/acs.nanolett.4c01364
7. Azari F, Zhang K, Kennedy GT, et al. Precision surgery guided by intraoperative molecular imaging. *J Nucl Med*. 2022;63(11):1620–1627. doi:10.2967/jnumed.121.263409
8. Jolugbo P, Willott T, Lin WH, et al. Fluorescent imaging using novel conjugated polymeric nanoparticles-affimer probes in complex in vitro models of colorectal cancer. *Nanoscale*. 2023;15(30):12476–12480. doi:10.1039/D3NR02160B
9. Lauwerends LJ, van Driel PBAA, Baatenburg de Jong RJ, et al. Real-time fluorescence imaging in intraoperative decision making for cancer surgery. *Lancet Oncol*. 2021;22(5):e186–e195.
10. Rainu SK, Ramachandran RG, Parameswaran S, Krishnakumar S, Singh N. Advancements in intraoperative near-infrared fluorescence imaging for accurate tumor resection: a promising technique for improved surgical outcomes and patient survival. *ACS Biomater Sci Eng*. 2023;9 (10):5504–5526. doi:10.1021/acsbiomaterials.3c00828
11. Liao XY, Liang SC, Liu YP, Zhang JY, Yan GP. Preparation, characteristics and cell imaging of fluorescent nanoparticles based on grafted poly (acrylic acid). *Chin J Anal Chem*. 2017;45(5):747–753.
12. Wysockia LM, Lavis LD. Advances in the chemistry of small molecule fluorescent probes. *Curr Opin Chem Biol*. 2011;15(6):752–759. doi:10.1016/j.cbpa.2011.10.013
13. Zhang X, Guo HZ, Chen CH, et al. Tunable photoacoustic and fluorescence imaging of nitrogen-doped carbon quantum dots. *Appl. Mater. Today*. 2023;30:101706.
14. Huang XL, Song JB, Yung BC, Huang XH, Xiong YH, Chen XY. Ratiometric optical nanoprobes enable accurate molecular detection and imaging. *Chem Soc Rev*. 2018;47(8):2873–2920. doi:10.1039/C7CS00612H
15. Liang SC, Liu YM, Fu T, Yang F, Chen XH, Yan GP. A water-soluble and biocompatible polymeric nanolabel based onnaphthalimide grafted poly (acrylic acid) for the two-photon fluorescence imaging of living cells and C. elegans. *Colloids Surf B*. 2016;148:293–298.
16. Liu F, Zou TJ, Tan ZL, et al. Isoindoline nitroxide-labeled porphyrins as potential fluorescence-suppressed spin probes. *Org Biomol Chem*. 2017;15:1245–1253.
17. Liu F, Zou TJ, Tan ZL, et al. Fullerenol spin probe containing isoindoline nitroxide and porphyrin groups. *FullerNanotub Car N*. 2016;24 (8):500–506.
18. Yan GP, Fairfull-Smith KE, Smith CD, Hanson GR, Bottle SE. Porphyrin containing isoindoline nitroxides as potential fluorescence sensors of free radicals. *J PorphyrPhthalocya*. 2011;15(4):230–239. doi:10.1142/S1088424611003203
19. Liu F, Shen YC, Ouyang YH, et al. Synthesis and properties of isoindoline nitroxides-containing porphyrins. *J Heterocycl Chem*. 2017;54 (6):3143–3151. doi:10.1002/jhet.2928
20. Mahounga DM, Shan LL, Jie C, Du CL, Wan SN, Gu YQ. Synthesis of a novel L-methyl-methionine–ICGDer-02 fluorescent probe for in vivo near infrared imaging of tumors. *Mol Imaging Biol*. 2012;14(6):699–707. doi:10.1007/s11307-012-0560-4
21. Giammona G, Carlisi B, Palazzo S. Reaction of α,β-poly(N -hydroxyethyl)- DL -aspartamide with derivatives of carboxylic acids. *J Polym Sci Polym Chem*. 1987;25(10):2813–2818. doi:10.1002/pola.1987.080251016
22. Giammona G, Pitarresi G, Pitarresi G, Carlisi B, Carlisi B. Coupling of the antiviral agent zidovudine to polyaspartamide and in vitro drug release studies. *J Control Release*. 1998;54(3):321–331. doi:10.1016/S0168-3659(98)00020-0
23. Yan GP, Liu ML, Li LY. Studies on polyaspartamide gadolinium complexes containing sulfadiazine groups as MRI contrast agents. *Bioconjugate Chem*. 2005;16:967–971.
24. Zhang M, Liu F, Ke XJ, et al. Polyaspartamide fluorescent probe containing rhodamine B and Sulfadiazine groups. *Chin J Org Chem*. 2020;40 (4):938–943. doi:10.6023/cjoc201908003
25. Zheng SY, Zhang M, Liu F, Yan GP, Liang SC, Wang YF. Dual-modal polypeptide-containing contrast agents for magnetic resonance/fluorescence imaging. *Bioorg Chem*. 2022;129:106127. doi:10.1016/j.bioorg.2022.106127
26. Liang SC, Liu YB, Xiang J, Qin M, Yu H, Yan GP. Fabrication of a new fluorescent polymeric nanoparticle containing naphthalimide and investigation on its interaction with bovine serum albumin. *Colloids Surf B*. 2014;116:206–210. doi:10.1016/j.colsurfb.2014.01.005
27. ZhaoJ J, Weng GJ, Li JJ, Zhu J, Zhao JW. Recent advances in activatable fluorescence imaging probes for tumor imaging. *Drug Discov Today*. 2017;22(9):1367–1374.
28. Zhu YL, Shen YC, Liu F, et al. Dual-modal fullerenolprobe containing glypican-3 monoclonal antibody for electron paramagnetic resonance/ fluorescence imaging. *FullerNanotubCar N*. 2021;29(4):280–287.
29. Wu Y, Cai WB, Chen XY. Near-Infrared fluorescence imaging of tumor integrin avβ3 expression with Cy7-labeled RGD multimers. *Mol Imaging Biol*. 2006;8(4):226–236. doi:10.1007/s11307-006-0041-8
30. Lolak N, Akocak S, Bua S, Sanku R, Supuran C. Discovery of new ureido benzene sulfonamides incorporating 1,3,5-triazine moieties as carbonic anhydrase I, II, IX and XII inhibitors. *Bioorg Med Chem*. 2019;27(8):1588–1594. doi:10.1016/j.bmc.2019.03.001

31. Meleddu R, Distinto S, Cottiglia F, et al. New dihydrothiazolebenzensulfonamides: looking for selectivity toward carbonic anhydrase isoforms I, II, IX, and XII. *ACS Med Chem Lett*. 2020;11(5):852–856. doi:10.1021/acsmedchemlett.9b00644
32. Huang JL, Wang HY, Zhou CL. Ring-opening polymerization of ethylene oxide by anioninitiation using sulfadiazine as parent compound. *J Appl Polym Sci*. 1995;58(8):–11. doi:10.1002/app.1995.070580102
33. Pal RR, Kim MS, Lee DS. Synthesis and pH-dependent micellization of sulfonamide-modified diblock copolymer. *Macrom Res*. 2005;13 (4):67–476.
34. Yan GP, Zheng CY, Cao W, et al. Synthesis and preliminary valuation of gadolinium complexes containing sulfonamide groups as potential MRI contrast agents. *Radiography*. 2003;9(1):3541. doi:10.1016/S1078-8174(03)00002-6
35. Liang SC, Yu H, Xiang J, et al. New naphthalimide modified polyethylenimine nanoparticles as fluorescent probe for DNA detection. *Spectrochim, Acta A Mol, Biomol, Spectrosc*. 2012;97:359–365. doi:10.1016/j.saa.2012.05.058
36. Liu F, Shen YC, Chen S, et al. Tumor-targeting fluorescent probe based on 1,8-naphthalimide and porphyrin groups. *Chemistryselect*. 2020;5 (26):7680–7684. doi:10.1002/slct.202001340
37. Shi FQ. How to copy the disease model of animals. In: *Medical Animal Experiment Method*. Vol. Chapter 4. Beijing, China: People's Medical Publishing House; 1990:226–232.